MM Science Journal | www.mmscience.eu
ISSN 1803-1269 (Print) | ISSN 1805-0476 (Online)
Special Issue | HSM 2021
16th International Conference on High Speed Machining
October 26-27, 2021, Darmstadt, Germany
DOI: 10.17973/MMSJ.2021_11_2021155

HSM2021-2021155

COMPARISON OF SPRAYABILITY AND SOLUBILITY OF BIO-BASED LUBRICANTS WITH LIQUID CARBON DIOXIDE

T. Meier[1]*, D. Gross[1], N. Hanenkamp[1]

[1]University Erlangen-Nuremberg, Institute for Resource and Energy Efficient Production Systems, Dr.-Mack-Str. 81, 90762 Fürth, Germany

*Corresponding author; e-mail: trixi.meier@fau.de

Abstract
In recent years, cryogenic minimum quantity lubrication (CMQL) has been established in comparison to pure cryogenic cooling. The used oil has a crucial influence on the success of the technology. The aim of this study is to investigate the influence of oils from renewable resources with regard to their miscibility with carbon dioxide (CO_2) and their spraying behavior. Ten different bio-based oils (synthetic ester, natural ester and fatty alcohol) have been examined regarding their suitability for CMQL compared to a conventional mineral hydrocrack oil. A validation based on sprayability and solubility properties with liquid CO_2 has been performed. The sprayability and the resulting oil droplet size have an impact on the amount of oil entering the process zone and thus on the lubrication performance of the coolant concept. For this reason, a high-speed camera has been used to capture shadow images of the jet from an external cooling nozzle. In addition the width, intensity and uniformity of the oil application were evaluated. The solubility of the bio-based oils in CO_2 is investigated in a static mixing chamber with varied mixing ratio. The miscibility of the bio-based oils in a single channel supply system was investigated with high-speed recordings of a dynamic mixing chamber. The results of the various experimental setups have been compared.

Keywords:
CMQL; milling; turning; bio-based oils; carbon dioxide

1 INTRODUCTION

Due to permanently increasing product complexity, growing global competitive pressure and higher quality requirements, new demands are constantly being placed on the performance of materials. The resulting high-performance materials can often only be machined at high economic and material cost using conventional manufacturing processes and cooling lubrication strategies. In addition, due to increasing sustainability efforts in industry and a changing environmental awareness, biological products are increasingly becoming the focus of current developments. [Murrenhoff 2010]

For these reasons, bio-based metalworking oils for cryogenic minimum quantity lubrication (CMQL) are investigated within this research to demonstrate their performance. Due to the cooling effect of the cryogenic medium, the process temperature in the cutting zone is reduced, which allows an increase of the cutting speed [Abele 2016]. Thus, the removal rate and the tool life can be improved in cutting processes compared to conventional flood cooling lubrication. In order to gain a more detailed understanding of the behavior of the two media liquid carbon dioxide (CO_2) and minimum quantity lubrication (MQL) oil in the supply line to the tool, the flowing medium is considered and analyzed in this work. The aim is to gain insights into the spray behavior at the nozzle outlet, the uniformity of the lubricant application, the static miscibility and the dynamic flow behavior.CO_2 and the biological lubricants also have the advantage, in contrast to other cooling lubricants, of producing less harmful vapors and thus pose a lower health risk to the machine operator [Sonnenberg 2016]. The ecological improvement of this concept is the main focus of this research.

2 STATE OF THE ART

The chapter provides an overview of the state of the art for cryogenic minimum quantity lubrication, the use of bio-based metalworking oils and the properties of the two media.

2.1 Cryogenic minimum quantity lubrication

In order to improve the lack of lubricity of pure cryogenic process cooling and the associated increased wear mechanisms, cryogenic cooling is combined with minimum quantity lubrication. CMQL covers all the main tasks of a cooling lubricant in machining: cooling, lubricating and flushing. The main cryogenic media used are nitrogen and carbon dioxide. In various studies, the focus is on the optimum process parameters for machining and influences on tool wear compared to conventional strategies.

[Su 2010; Pereira 2015; Bagherzadeh 2018; Zhang 2018; Gross 2019a; Gross 2019b; Gross 2020]

The cryogenic medium (the carrier) and the lubricant can be fed to the processing zone via two different systems. Either via a two-channel system or via a single-channel supply system. With a two-channel system both media are transported separately from each other and also sprayed separately to the process area. During the spraying process, the two substances are partially mixed, which ultimately results in both a cooling and a lubricating effect. Since the physical and chemical correlation of the carrier medium with the lubricant in the feed line does not play a role in this feed variant, more investigations have so far been concerned with the two-channel system. It is significantly less complex than the single-channel system. [Duchosal 2015; Pereira 2015; Pereira 2016]

In a single-channel system, both substances are fed to the process zone as a mixture, as in MQL. Within these tests, the CO_2 is taken directly in the liquid state from a pressure vessel and the lubricant is continuously pumped into the carrier medium. The mixture is transported in a pressure line to the processing point and sprayed into the process zone with an aligned nozzle or through channels inside the tool [Hanenkamp 2018]. It is essential to know how the two media behave in the common feed channel and which properties of the oil can lead to the best performance for machining.

2.2 Properties of carbon dioxide

Carbon dioxide, with the molecular formula CO_2, consists of a carbon atom to which two oxygen atoms are bonded, each with a double bond. It is a colorless, odorless and non-flammable gas and a natural component of air, with a concentration of 0.04%. Due to its molecular symmetry, it is non-polar. Huge amounts of CO_2 are produced in industry, especially during combustion processes. In processes with increased CO_2 emissions, such as in power plants, absorption-desorption processes are used to chemically remove the CO_2 from the exhaust gases and treat it. The gas, which is still in gaseous form, can be liquefied in large quantities using the "Linde process," for example. The gas passes through the same process several times, during which it is compressed, cooled and expanded. [Fischedick 2015]

Carbon dioxide exists in the gaseous state at room pressure and temperature. The states of the substance as a function of pressure and temperature are shown either in a P-V or in a P-T phase diagram, Fig. 1.

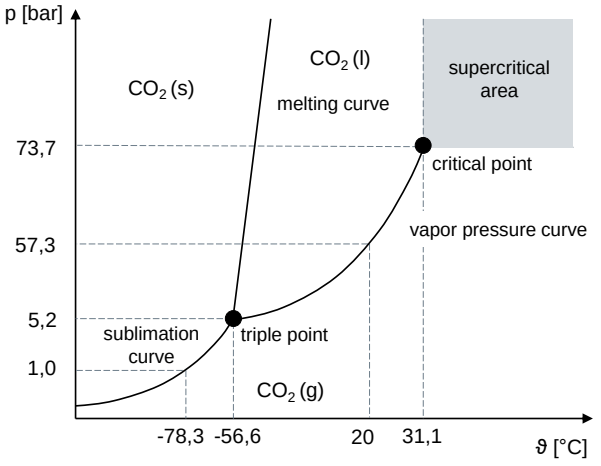

Fig. 1: PT-diagram of CO_2 [Kabelac 2006; Krämer 2015].

The state of CO_2 is indicated by: solid (s), liquid (l) and gaseous (g). The triple point represents a state where the pressure and temperature keep all three phases in a thermodynamic equilibrium. Consequently, at this point, the substance can exist in any of the three phases simultaneously. The supercritical region (also called the transcritical region) is similar. From the critical point onwards, both states form a uniform common phase, which visually resembles a liquid phase, but has a significantly lower surface tension and viscosity as well as a higher diffusivity (spreading of a solute). In this range, CO_2 has very good dissolving properties for non-polar substances, which is why it is mainly used for the extraction of organic substances. The phase diagram can be used in particular to describe the thermodynamic processes during the exit of the LCO_2 from the nozzle. Inside the pipe and the pressure bottles, it is in the liquid state due to the vapor pressure of P_D = 57.3 bar at roomtemperature (ϑ_1 = 20 °C). The liquid and gaseous phases are in phase equilibrium within the pressure vessel. The exit mechanisms at the free jet nozzle were investigated in 2012 by Mark Pursell of the Health and Safety Laboratory in Buxton (UK). According to this study, several thermodynamic mechanisms ensure cooling of the gas and the environment in the outlet area of the nozzle. Each substance, even if it is already at the boiling point, requires a substance-specific heat of vaporization to change its aggregate state from liquid to gas. This separation work is necessary to overcome the attractive forces between the molecules, such as the Van der Waals forces or the dipole moments. For CO_2, this requires an energy of ΔQ = 573.02 kJ/kg, which is taken from the thermal energy of the liquid phase. According to Pursell, approx. 14 to 16 mass-% of the liquid phase passes into the gaseous phase. Due to the pressure gradient to the ambient pressure, the gas expands and cools further due to the Joule-Thomson effect. When the triple point is reached at p_t = 5.18 bar and ϑ_t = -56.56 °C, the remaining liquid CO_2 converts to the solid state and sublimates along the sublimation curve up to ambient pressure to a temperature ϑ = -78.3 °C. [Kabelac 2006; Pursell 2012]

2.3 Biobased lubricants

Biological cooling lubricants represent an environmentally compatible and regenerative alternative to conventional mineral oils based on petroleum. According to the recommendation of the German Institute for Standardization (DIN), biolubricants are defined in "DIN CEN/TR 16227 2011" as substances which originate from at least 25% renewable raw materials, are more than 60% biodegradable and are not classified as environmentally hazardous [DIN CEN/TR 16227 2011]. Extending this, there is the general classification of lubricants into biobased and biodegradable. Bio-based in this case refers to the regenerative origin, such as vegetable oils. However, these can still contain performance-enhancing toxic additives and are not necessarily biodegradable.

2.4 Properties of triglycerids

Since triglycerides belong to the lipids, they combine several properties. They are basically hydrophobic and have a very low polarity. Often, oils are also described as non-polar. Due to the composition of the triglyceride from different fatty acids, certain properties are strengthened or weakened by them, as it is described in the following sections.

Polarity refers to the presence of separate centers of charge in the molecule and thus whether or not the atomic group has electrical neutrality. In general, when solving substances with respect to polarity, the guiding principle is "like in like." This means that substances with the same

polarity dissolve in each other until saturation and form a homogeneous phase. [Latscha 2016]

Depending on the composition (number of C-atoms, position of the double bond, etc.) and the position of the fatty acids on the glycerol, different physical and chemical properties result. In general, long-chain and saturated fatty acids increase the viscosity of the triglyceride. In contrast, oils with short unsaturated fatty acids have a lower melting point. This is also the reason for the difference between fats with a melting point above room temperature and oils with a melting point below room temperature. Fats can therefore always be converted into oils by adding thermal energy. [Behr 2018; Lipid 2020]

As already described, saturated fatty acids are less reactive than unsaturated ones, which is why they have less influence on the chemical properties of the oil. If, on the other hand, an oil consists largely of polyunsaturated carboxylic acids, such as alpha-linolenic acid (18:3), it often tends to oxidize. Monounsaturated fatty acids, such as oleic acid (18:1), which is the largest component in canola oil, sunflower oil and olive oil, cause less severe oxidation reactions. Oleic acid gives the oil slightly amphiphilic (literal meaning: "both loving") properties. It has both hydrophobic and hydrophilic (water-loving) properties. Similar to oils with a high erucic acid content (22:1), this results in less poor water solubility. [Latscha 2016; Behr 2018]

Since the various fatty acids are studied and characterized almost exclusively with regard to the medical field, food chemistry and for the production of biofuels, no other biobased oil properties relevant for CMQL could be determined on the basis of the fatty acids in the course of the research. Although a study by the Brazilian University of Blumenau comprehensively summarizes the properties of regenerative oils, it refers exclusively to relevant variables for biodiesel production. Thus, properties such as water content, oxygen content, dynamic viscosity or calorific value were mainly collected. [Stedile 2015]

2.5 Solubility in general

Since the solubility behavior of LCO_2 with various vegetable oils and synthetically produced esters will be studied in this work, among other things, the general solubility mechanisms are described in this section. In general, solutions are homogeneous mixtures of a solvent (dispersant) and a solute (disperse phase). The solubility indicates the maximum mass of substance that can dissolve in the dispersant. It is given as the mass concentration c_L in mol/l, or as the mass concentration $ß_L$ in g/l. This maximum concentration is substance-specific. For thermodynamic reasons, when two gaseous or liquid phases come into contact, part of each phase always dissolves in the other. The solubility depends on the polarity, i.e. the internal charge of the substance. Polar substances therefore dissolve in polar solvents and vice versa. The more the polarity of the two substances differs, the less easily they dissolve in each other. [Czeslik 2010]

The maximum concentration depends not only on the polarity but also on the substance temperature. High temperatures increase the solubility of solids and liquids, but reduce the solubility of gaseous substances in liquid solvents. Once the maximum concentration is reached, the solution is saturated. From this point on, the two substances no longer dissolve in each other and form two separate phases with a thermodynamic equilibrium. Before this point, the mixture forms a single-phase homogeneous mixture. The dependence of the soluble miscibility ratio of two liquid phases with temperature is shown in T-x phase diagrams. Since two liquid substances often only dissolve proportionally in each other, so-called miscibility gaps occur in some mixtures. It's called a miscibility gap when a substance ratio occurs in which no homogeneous mixture is formed. Like solubility, this gap is temperature-dependent. Fig. 2 shows two exemplary T-x diagrams (also called segregation diagrams). These show the areas where complete mixing of the two substances is possible (1) and the areas where two phases are formed (1'+1''), where both substances are saturated with the other. UCST indicates the critical segregation temperature, which is the temperature above which segregation is canceled. Conversely, LCST indicates the critical temperature above which the miscibility gap closes. [Czeslik 2010]

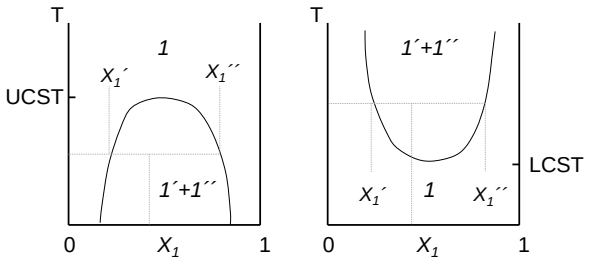

Fig. 2 : T-x diagrams to show the segregation of a mixture [Czeslik 2010].

In his dissertation, however, Jörg Fahl recognizes that the interactions between lubricating oils and CO_2 are not determined by polarity or permittivity (polarizability) alone, but also depend to a large extent on the structure of the lubricating oils. It describes the analysis of the suitability of various base oils of different chemical groups as lubricating oils for CO_2 refrigeration systems and relates primarily to the use of the refrigerant in automobiles, but also to deep-freeze systems. In addition to the bonding properties of the lubricating oils with CO_2, he also investigates the tribological properties, such as frictional behavior and wear of the oil-CO_2 mixture in the subcritical and transcritical range. Finally, he divides the test oils into three groups that describe their suitability as low-temperature lubricating oils. Class A describes oils with comparatively poor solubility. Class B includes those oils that exhibit partial miscibility in the temperature range (ϑ_1 = 0 °C to ϑ_2 = 120 °C) and pressure range (p = 30 bar to p = 140 bar) of an automotive air conditioning system. Aliphatic carboxylic acid esters, which also include triglycerides, are classified by him in class B. In class C, oils with good miscibility, even in the low temperature range up to ϑ = -55 °C. However, he does not publish an exact value for the solubility concentration or a T-x diagram. [Fahl 2002]

Grguras describes in the article « A novel cryogenic machining concept based on a lubricated liquid carbon dioxide » investigations on a single channel system for CMQL with CO_2. Miscibility tests of LCO_2 and base mineral oils and special MQL oils are carried out at a mixing ratio of 1:9. The evaluation here is purely qualitative with the statement whether the oil dissolves in LCO_2 at ϑ = 20 °C and p = 57 bar or not. It is found that both non-polar test oils dissolve completely in the solvent and the polar ones remain undissolved in the pressure chamber. In addition, spray tests and oil application tests are also carried out. [Grguras 2019]

In « Investigation of the solubility of liquid CO2 and liquid oil to realize an internal single channel supply in milling of Ti6Al4V », he also addresses the issue of miscibility of carbon dioxide and oil. The solubility of two mineral oil based lubricating oils in LCO_2 is investigated. In this investigation, the oil to carbon dioxide ratios are varied to 50:50, 75:25 and 25:75. [Bergs 2019]

2.6 Flow types

The flow behavior of the mixture of LCO_2 and varying lubricants is to be investigated in experiments with the high-pressure viewing cell. Idealized, a pure liquid flow in a pipe has a parabolic velocity profile, with a slower turbulent flow near the edge and an inner laminar faster flow [Bschorer 2018]. In this consideration, however, there is a pure liquid substance without a vapor component. Depending on the substance, temperature, pressure and surface of the pipeline, however, real flows usually consist of a proportion of gaseous phase. This results in different flow forms. Due to gravity, the resulting shapes differ significantly in vertical and horizontal pipes. In these, the VDI defines six flow forms for vertical pipes and seven for horizontal pipes. Accordingly, in horizontal pipes a bubble, plug, stratified, wave, surge, annular or mist flow can occur. Whereby the types overlap in the boundary areas and can thus occur simultaneously. [Kabelac 2006]

3 EXPERIMENTAL SETUP

The following chapter describes the experimental setup and the execution of the individual experiments.

3.1 Cryogenic mixing unit and biobased oils

In the experiments, the influence of ten bio-based base oils on sprayability and miscibility with cryogenic minimum quantity lubrication is investigated. Various unadditivated biobased base oils from three lubricant manufacturers are selected for the tests. A hydrocrack mineral oil, also unadditivated, is examined as a reference and the results are compared. The relevant chemical properties and the associated measurement methods are determined for the selection of the oils. In order to comply with the competitive secrets of the individual lubricant manufacturers, value ranges are defined seperately for each property, and the selected oils cover all defined ranges. This is shown in the Tab. 1 below.

Tab 1: characteristics and value areas of test oils.

characteristic	measuring method	value areas	*unit*
viscosity 40	Stabinger	<10	*mm²/s*
		10 - 20	
viscosity 100	Stabinger	<2	*mm²/s*
		2 - 5	
viscosity index	Stabinger	<90	
		120 - 150	
		>150	
densitiy (15°C)	DIN 51757	< 0,08	*g/ml*
		0,08 - 0,09	
		> 0,9	
chain length (number of c-atoms)		< C10	
		C10 - C20	
		> C20	
polarity	Non Polarity Index	nonpolar	
		weak polar	
		polar	
pourpoint	DIN ISO 3016:2017	> -50	*°C*
		-50 to -80	
		< -80	
ester content		0	*%*
		> 95	
water content	DIN 51777-1	< 0,05	*%*
		0,05-0,1	
sulfur content	DIN 51399-1 ICP	< 0,01	*%*
phosphor content	DIN 51399-1 ICP	< 0,01	*%*

The following Tab. 2 contains the abbreviation of the respective oils and additionally its chemical structure and the content of renewable crude rawmaterial.

Tab. 2 : chemical structue and RRM content of test oils.

name	chemical structure	RRM content (Renewable Rawmaterial)
SE 1	monoester	75 - 99%
SE 2	azelaic acid ester	25 - 50%
SE 3	monoester	100%
SE 4	dicarboxylic acid esters	< 40%
SE 5	monoester	> 50%
SE 6	polyolester	> 80%
NE 1	triglyceride	100%
NE 2	triglyceride	100%
NE 3	triglyceride	100%
KW 1	-	75 - 99%
KW 2	hydrocrackoil	0%

SE: synthetic ester **FA:** fatty alcohol
NE: natural ester **KW:** natural hydrocarbon

The mixing system developed at the Institute REP [Hanenkamp 2018] is used for this purpose, Fig. 3. The volume flow of the oil is regulated in the CMQL system of the chair by controlling a HPLC pump. The mass flow of the LCO_2 is measured by a Coriolis sensor and shown on a display. This also shows the temperature and density of the medium. The pump system consists of the Coriolis sensor, an analog barometer, a thermometer and shut-off valves for the carbon dioxide and oil supply. The liquid CO_2 is taken from a CO_2-bundle with riser bottles.

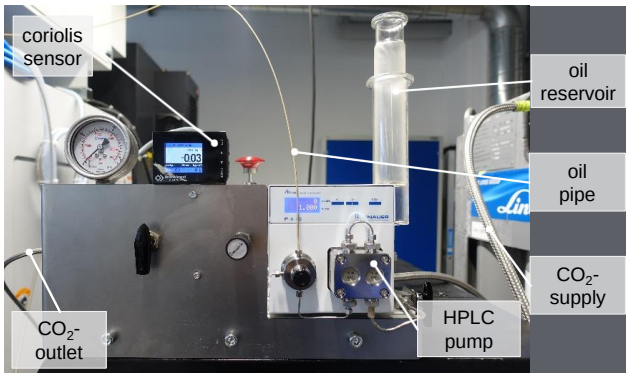

Fig. 3 : cryogenic mixing unit.

3.2 Spray pattern investigations

The spray image tests are recorded using an ultra-high-speed camera FASTCAM SA-Z from the manufacturer Photon via shadow light recording. This allows a maximum frame rate of 54000 fps (frames per second) at a resolution of 768 x 512 pixels. In the experiment, the frame rate is set to 40000 fps. 2000 frames are recorded, which corresponds to a real time of 0.05 s. The experimental setup is shown in the figure 4. The free-jet nozzle is a round nozzle with an outlet diameter of d = 0.2 mm and is aligned horizontally in the present experiment. The oil flow rate is V = 0.8 ml/min in all experiments. The mixing system, the piping and the LCO_2 supply is identical to the setup of the oil application test.

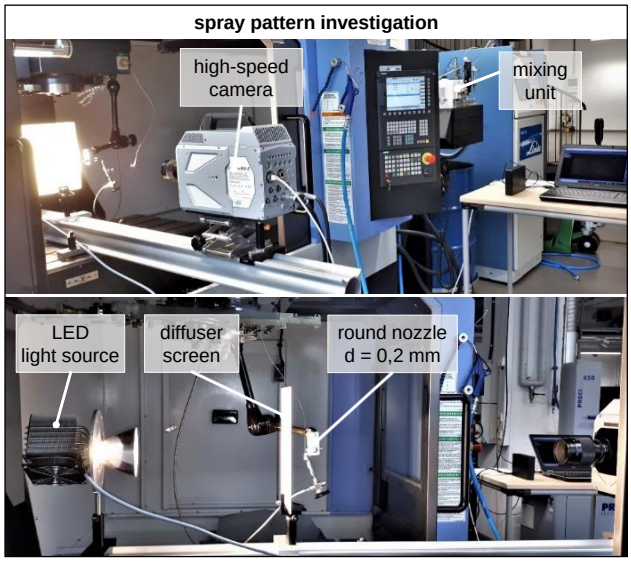

Fig. 4: experimental setup spray pattern investigation.

3.3 Oil application tests

The second test carried out is the oil application test, in which the uniformity of the lubricant application through the identical round free-jet nozzle is to be investigated. The application pattern of the oil is made visible with the aid of blotting paper. In order to achieve a constant and repeatable nozzle movement with a feed rate (v_f = 2000 mm/min), the test is carried out in the milling machine. The nozzle is aligned pointing downward at a distance of Δz = 40 mm from the machine table, see Fig. 5. This is the optimum distance determined in preliminary tests for external cooling when milling with CMQL. The LCO_2 mixing system is connected to the nozzle. During the experiment, the HPLC Pumoe delivers a volume flow of V = 0.8 ml/min of the respective test oil. After the test has been carried out, the oil application is immediately recorded with a camera.

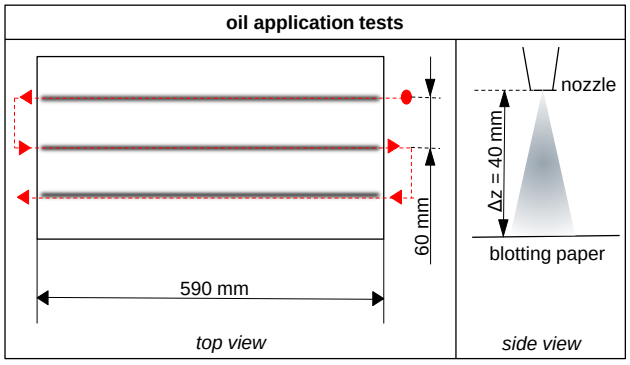

Fig. 5 : experimental setup oil application tests.

3.4 Static miscibility tests

The static high-pressure viewing cell used in this experiment was developed at the REP Chair. The complete experimental setup is shown in Fig. 6. The cell consists of a high-pressure mixing chamber with a volume of V = 1 ml, which is equipped with an optical sight glass on both sides. A T-screw fitting is firmly attached to the lid of the mixing chamber. On the one hand, a HPLC pump is connected to it and, on the other hand, an LCO_2 supply line from a riser bottle. The chamber is filled with oil with Voil = 0.2 ml, with liquid CO_2 with $VCO_{2(l)}$ = 0.7 ml and gaseous CO_2 with $VCO_{2(g)}$ = 0.1 ml and then the supply channels are closed. The gaseous phase and thus the visible boundary between gaseous and liquid CO_2 is considered as proof that liquid CO_2 is really present in the visible cell.

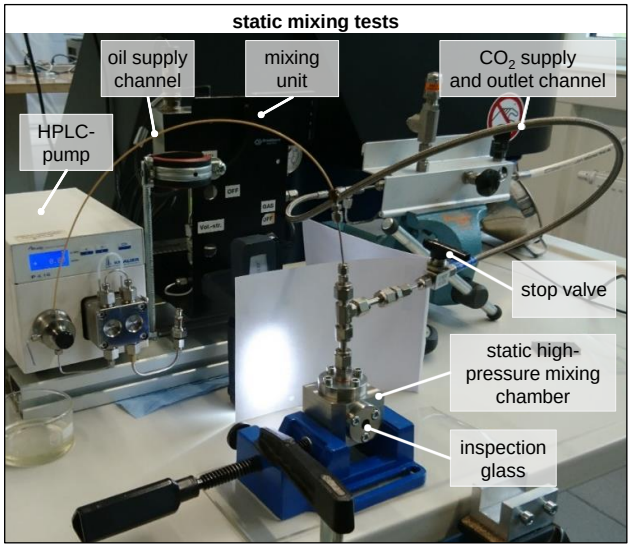

Fig. 6: experimental setup static mixing tests.

To accelerate the solution reaction, the chamber is removed from the vice and shaken by hand for about ten seconds. This increases the interface area, which increases the reaction rate. However, since in the CMQL the oil is added to the LCO_2 stream immediately upstream of the nozzle, leaving little time for a mixing reaction, the experiment is a realistic representation of the mixture in the line. After the shaking process, the result is documented by camera.

3.5 Dynamic miscibility tests

In the dynamic mixing test, the flow behavior of the LCO_2 oil mixture of the different test oils is investigated. In addition, the investigations are to be used to draw conclusions about previously unexplained effects of the other tests. To this end, a realistic operating condition for the supply of CMQL during machining is simulated with the test setup shown, using a high-pressure viewing cell, developed in-house at the REP-Chair, for a flowing fluid. With the aid of the high-pressure viewing cell, the behavior of the CO_2-oil mixture in the single-channel feed can be observed optically. The viewing cell is operated at an operating pressure of p = 57.3 bar, as CMQL is used for machining. The experimental setup is shown in Fig. 7.

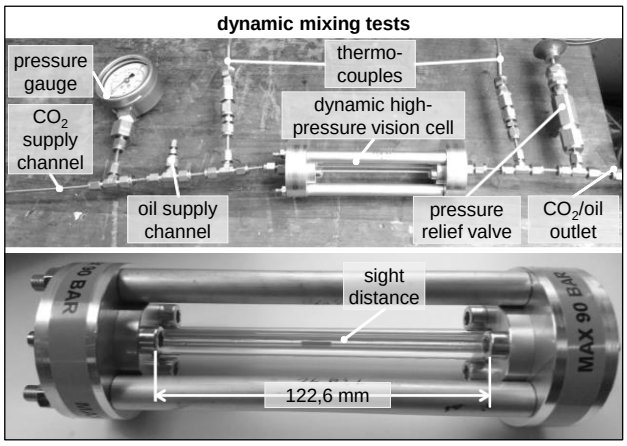

Fig. 7 : experimental setup dynamic mixing tests.

In addition to the high-pressure cell, it includes a pressure indicator, temperature measurement upstream and downstream of the cell, and a pressure relief valve. This ensures the operational safety of the glass capillaries with

sufficient reliability. A round nozzle with a diameter of d = 0.2 mm is again connected to the discharge side. A high-speed camera of the model series VW9000 of the manufacturer KEYENCE with illumination unit and zoom is used for the exact observation of the flow. The images are taken with the following settings: an exposure time of 1/900000 seconds, a frame rate of 10000 fps and an image resolution of 640 x 192 pixels.

4 RESULTS

4.1 Spray pattern investigations

In order to create a basis for the evaluation, a reference exposure without oil is first carried out with this setup. In addition to the camera images, the observable effects, such as the development of fog, are also noted for all runs. The beam uniformity, the characteristics of the beam elements (main beam, steam behind and mist in the processing chamber) and any special deviations are evaluated.

Low jet uniformity occurs with an LCO_2 oil mixture with the test oils NE 1 and NE 3. With these oils, pulsating droplet emissions can be observed at irregular intervals, Fig. 8. In the case of NE 3 in particular, these point obliquely downwards and may therefore not reach the processing zone to which the nozzle is directed. A uniform jet pattern with a visible main jet length of approx. 40 mm and low oil vapor development behind the main jet is achieved by most of the oils. The oils NE 2, KW 1 and KW 2 show a uniform jet pattern with a main jet length of approx. 60 mm and medium to strong oil vapor development behind the main jet.

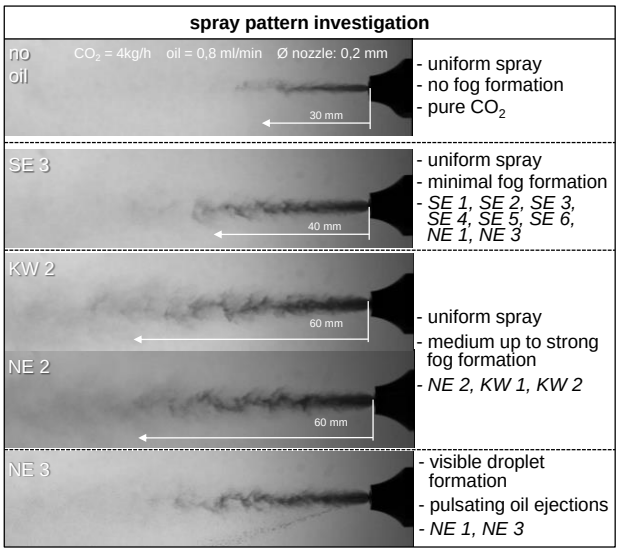

Fig. 8: results spray pattern investigation.

Finally, a consideration of the mist development in the machining area takes place, which is relevant as soon as the lubricant is used in longer machining processes. The development of mist causes several disadvantages: deterioration of visibility in the machining area (not relevant to the process), distribution of the oil in the entire machining area and thus contamination of the entire area, aerosols remain in the air for a long time (possible health risk for machine operators when changing workpieces or tools). As a countermeasure, a more powerful extraction system is necessary.

A strong mist or aerosol formation can only be seen with the oils NE 2, SE 4 and KW 1, and a medium mist with the oils SE 1, SE 2, SE 5 and SE 6. No mist is formed with the remaining oils and with the reference. An overview of this is shown in Fig. 9. However, a correlation between the vapor development behind the main jet and the fogging or aerosol formation in the machine is not clearly recognizable. An example of this is KW 2.

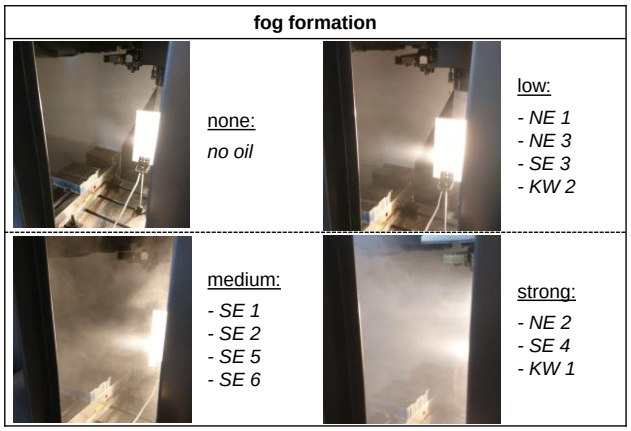

Fig. 9: fog formation.

4.2 Oil application tests

When evaluating the tests, the following properties are examined: uniformity of the application pattern, intensity of the oil application, width of the oil application, frequency of the drops, size of the drops, streaking due to icing and the formation of ice.

Particularly in the case of the NE 1, NE 3, SE 1 and SE 2 oils, a high degree of uniformity in the oil application can be seen, Fig. 10. This indicates a high level of process reliability. In addition, a high application intensity is observed with the NE 1 and NE 3 oils. This directed concentrated oil application, with a simultaneously small application width, is advantageous for the CMQL, since on the one hand the lubricant is distributed little in the edge areas or within the machining area as a mist. On the other hand, it can be assumed that more oil hits the machining zone in order to lubricate there and, at best, evaporate without leaving residues.

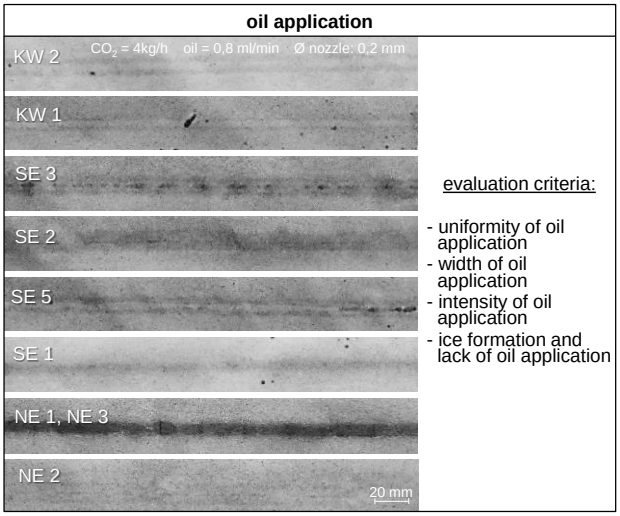

Figure 10 : oil application results.

Furthermore, during these tests, it was documented whether a layer of ice had formed on the application surface and, if so, this was related to the oil application pattern. If ice formation could be recorded but no oil application was visible in the center of the oil application tests, it can be concluded that no oil was dissolved in the CO_2 snow and that it was only deposited at the edge, see sketch in Fig. 11. However, in the case of strong ice formation and intensive

oil application in the center, it can be assumed that oil was present in the CO_2 snow.

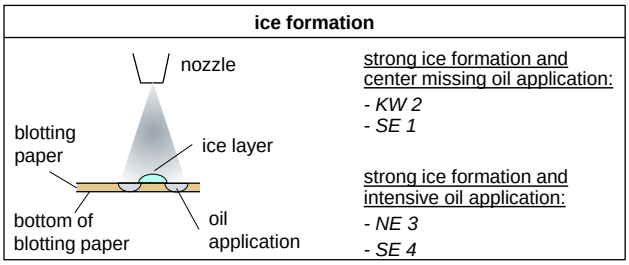

Fig. 11: ice formation during oil application tests.

4.3 Static miscibility tests

In the static mixing test, the miscibility properties of the oils are analyzed with LCO_2 in a static pressure chamber with sight glass. After shaking, as described in the test setup, four different result cases occur. The test oils can be divided into category 1: solubility of CO_2 in oil, category 2: solubility of oil in CO_2, category 3: complete solubility and category 4: no solubility. The results are shown in Fig. 12.

In particular, the oils SE 1 and SE 5 stand out due to their complete solubility. Half of the oils investigated fall into the category 4 no solubility. In the case of SE 6 and NE 2, CO_2 dissolves in the oil, and in the case of the hydrocarbons, the oil dissolves only partially in liquid CO_2.

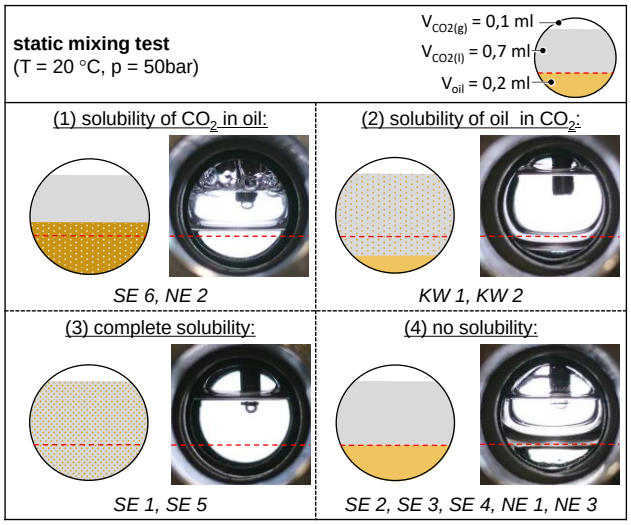

Fig. 12: results static mixing test.

4.4 Dynamic miscibility tests

The experiment starts with a reference recording of the flow without oil. Without oil, the LCO_2 forms a surge flow. If oil is added to the carbon dioxide, the shape changes to a kind of bubble flow, Fig. 13. In addition, a milky turbidity of the fluid can be seen in the real-time observation of the test. Basically, with all test oils, the droplet or bubble density increases, producing a more blurred and darker slow-motion image. A two-phase mixture is formed in the line in which the oil is carried along by the carbon dioxide in many small droplets. In the case of oil SE 3 and the natural esters NE 1 and NE 3, a sawtooth-shaped oil deposit is conspicuous in the lower region of the line. This moves much slower than the rest of the stream. A rough calculation using uptake and particle tracking shows that this laminar boundary layer moves about ten times slower than the central stream. The flow test also allows an explanation of the shock-like oil ejections observed in the spray test for the NE 1 and NE 3 oils. If the oil layer moves toward the nozzle, the individual elevations generate an uneven oil ejection. If a particularly large oil layer forms in the nozzle area, it is ejected in a bundled jet. In the case of SE 3, however, this effect is not discernible in the dynamic mixing test. A surprising observation is also made in tests with the oils SE 1 and SE 5, which exhibit complete solubility in LCO_2 in the static miscibility test. However, in the flow test, no difference can be observed between these two oils and the other oils.

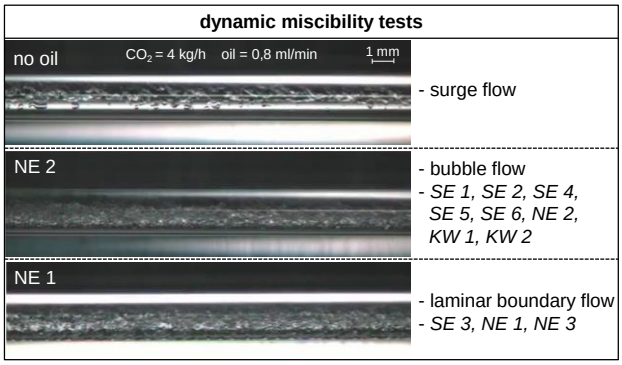

Figure 13 : results dynamic miscibility tests

5 SUMMARY

In summary, the development of static and dynamic high-pressure vision cells has made it possible to explain some of the results and effects of the spray pattern and oil spreading studies. In particular, the visible pulsating oil discharges at NE 1 and NE 3. However, not all results correlate. In particular, the complete solubility in the static cell for the oils SE 1 and SE 5 could not be demonstrated under dynamic conditions.

This study shows that the selected oils have an influence on the sprayability and miscibility. With the aid of the test setups described here, correlations with tool life machining investigations are to be established in the future. From this, cause-effect relationships are to be developed which can enable a statement to be made in advance about the possible performance of the oil in order to be able to reduce time-consuming and cost-intensive series of tests on machine tools.

6 ACKNOWLEDGMENTS

The results are part of the research project « ECO_2il - Development of bio-based metalworking oils for croygenic minimum quantity lubrication ». Thanks go to the German Agency for Renewable Resources and the German Federal Ministry of Food and Agriculture for funding the joint project. The consortium of the individual sub-projects consists of one research institution (REP-Chair of FAU Erlangen-Nuremberg), three end-user companies (Gühring KG, EagleBurgmann Germany GmbH & Co. KG, Schaeffler AG) and three lubricant manufacturers (Fuchs Schmierstoffe GmbH, Rhenus Lub GmbH & Co KG, Blaser Swisslube GmbH).

7 REFERENCES

[Abele 2016] Abele, E. and Scherer, T. Den Verschleiß kaltgestellt. WB Werkstatt+Betrieb, 2016.

[Bagherzadeh 2018] Bagherzadeh, A. and Budak, E. Investigation of machinability in turning of difficult-to-cut materials using a new cryogenic cooling approach. Tribology Internationa,l Vol. 119, 2018, pp. 510–520.

[Behr 2018] Behr, A. and Seidensticker, T. Einführung in die Chemie nachwachsender Rohstoffe. Vorkommen, Konversion, Verwendung. Berlin and Heidelberg, 2018.

[Bergs 2019] Bergs, T., et al. Investigation of the Solubility of Liquid CO2 and Liquid Oil to Realize an Internal Single Channel Supply in Milling of Ti6Al4V. Procedia Manufacturing, Vol. 33, 2019, pp. 200–207.

[Bschorer 2018] Bschorer, S. and Buck, T. Technische Strömungslehre. Wiesbaden, 2018.

[Czeslik 2010] Czeslik, C., et al. Basiswissen Physikalische Chemie. Wiesbaden, 2010.

[DIN CEN/TR 16227 2011] DIN CEN/TR 16227, DIN SPEC 51523:2011-10. Flüssige Mineralöl-Erzeugnisse - Bio-Schmierstoffe - Empfehlungen für die Terminologie und Charakterisierung von Bio-Schmierstoffen und biobasierten Schmierstoffen, 2011.

[Duchosal 2015] Duchosal, A., et al. Numerical modeling and experimental measurement of MQL impingement over an insert in a milling tool with inner channels. International Journal of Machine Tools and Manufacture, Vol. 94, 2015, pp. 37–47.

[Fischedick 2015] Fischedick, M., et al. CO2. Abtrennung, Speicherung, Nutzung. Ganzheitliche Bewertung im Bereich von Energiewirtschaft und Industrie. Berlin, 2015.

[Fahl 2002] Fahl, J. Entwicklung und Erprobung von Schmierölen für Kälte- und Klimasysteme mit CO2 als Arbeitsstoff. Fakultät für Maschinenbau, Ruhr-Universität Bochum, 2002.

[Grguras 2019] Grguras, D., et al. A novel cryogenic machining concept based on a lubricated liquid carbon dioxide. International Journal of Machine Tools and Manufacture, 2019.

[Gross 2019a] Gross D., et al. Investigation of the influence of lubricating oils on the turning of metallic materials with cryogenic minimum quantity lubrication. Procedia CIRP, Vol. 80, 2019, pp. 95-100.

[Gross 2019b] Gross D., et al. Investigation on the productivity of milling Ti6Al4V with cryogenic minimum quantity lubrication, MM Science Journal, 2019, pp. 3393-3398

[Gross 2020] Gross D., et al. Milling of Ti6Al4V with carbon dioxide as carrier medium for minimum quantity lubrication with different oils. Procedia Manufacturing, Vol. 43, 2020, pp. 439-446

[Hanenkamp 2018] Hanenkamp N., et al. Hybrid Supply System for Conventional and CO2/MQL-based Cryogenic Cooling. Procedia CIRP, Vol. 77, 2018, pp. 219-222.

[Kabelac 2006] Kabelac, S. VDI-Wärmeatlas. Berechnungsunterlagen für Druckverlust, Wärme- und Stoffübergang. Berlin and Heidelberg, 2006.

[Krämer 2015] Krämer, A. Gestalltungsmodell der kryogenen Prozesskühlung in der Zerspanung. Aachen, RWTH-Aachen. Dissertation. 2015.

[Latscha 2016] Latscha, H. P. et al. Organische Chemie. Chemie-Basiswissen. Berlin and Heidelberg, 2016.

[Lipid 2020] LIPID MAPS. LIPID MAPS® Lipidomics Gateway, 2020, available at: http://www.lipidmaps.org/resources/lipidweb/index.php?page=lipids/lipids.html, date last checked 29.06.2020.

[Murrenhoff 2010] Murrenhoff, H. Umweltverträgliche Tribosysteme. Die Vision einer umweltfreundlichen Werkzeugmaschine. Berlin and Heidelberg, 2010.

[Pereira 2015] Pereira, O. et al. The Use of Hybrid CO2+MQL in Machining Operations. Procedia engineering, Vol. 132, 2015, pp. 492–499 .

[Pereira 2016] Pereira, O., et al. Cryogenic and minimum quantity lubrication for an eco-efficiency turning of AISI 304. Journal of Cleaner Production, Vol. 139, 2016, pp. 440–449.

[Pursell 2012] Pursell, M. Experimental investigation of high pressure liquid CO2 release behaviour. Symposium Series, Vol. 158, 2012.

[Sonnenberg 2016] Sonnenberg, V. Mit kryogener Bearbeitung zu einer effektiveren und umweltfreundlicheren Zerspanung. Maschinenmarkt, 2016.

[Stedile 2015] Stedile, T., et al. Comparison between physical properties and chemical composition of bio-oils derived from lignocellulose and triglyceride sources. Renewable and Sustainable Energy Reviews, Vol. 50, 2015, pp.. 92–108.

[Su 2010] Su, Y., et al. Effect of Cryogenic Minimum Quantity Lubrication (CMQL) on Cutting Temperature and Tool Wear in High-Speed End Milling of Titanium Alloys. Mechanical Engineering and Green Manufacturing, Vol. 34, 2010, pp. 1816–1821.

[Zhang 2018] Zhang, H. P. et al. Simulation and Experiments on Cutting Forces and Cutting Temperature in High Speed Milling of 300M Steel under CMQL and Dry Conditions. International Journal of Precision Engineering and Manufacturing, Vol. 19, No. 8, 2018, pp. 1245–1251.